Liquid Crystals
Publication details, including instructions for authors and subscription information:
http://www.informaworld.com/smpp/title~content=t713926090

Rigorous calculation of pixel and inter-electrode capacitances of thin-film transistor liquid crystal displays using three-dimensional simulation

Sung-Min Jung[a]; Woo-Sang Park[a]
[a] School of Electrical & Computer Engineering, Inha University, 253 Yonghyun-dong, Nam-ku, Inchon 402-751, Korea,

Online publication date: 11 November 2010

To cite this Article Jung, Sung-Min and Park, Woo-Sang(2003) 'Rigorous calculation of pixel and inter-electrode capacitances of thin-film transistor liquid crystal displays using three-dimensional simulation', Liquid Crystals, 30: 1, 1 — 5
To link to this Article: DOI: 10.1080/0267829021000018077
URL: http://dx.doi.org/10.1080/0267829021000018077

LIQUID CRYSTALS, 2003, VOL. 30, NO. 1, 1–5

Rigorous calculation of pixel and inter-electrode capacitances of thin-film transistor liquid crystal displays using three-dimensional simulation

SUNG-MIN JUNG and WOO-SANG PARK*

School of Electrical & Computer Engineering, Inha University,
253 Yonghyun-dong, Nam-ku, Inchon 402-751, Korea

(*Received 15 March 2002; accepted 26 June 2002*)

We have rigorously calculated for the first time all the inter-electrode and pixel capacitances of Thin-Film Transistor Liquid Crystal Displays using the electrical energy distribution inside a liquid crystal cell. The energy distribution is obtained from the three-dimensional profiles of potential distribution and molecular director. The dynamic equation of continuum theory for liquid crystals is described in a tensorial form in order to maintain the equivalence of **n** and $-\mathbf{n}$. The effects of lateral fields generated by multiple electrodes of finite sizes are taken into account in the simulation. As a numerical technique, we used a finite difference method which is suitable for the highly non-linear equations. As a result, we confirmed that the pixel capacitance for our pixel structure is about 40% larger than that of the conventional approach. It is also revealed that the gate-common and gate-data inter-electrode capacitances are not negligible.

1. Introduction

Recently, as the applications of thin-film transistor liquid crystal displays (TFT-LCDs) have extended to high-quality TVs and monitors, mobile displays, and micro-projection systems, the demand for fine pitch and high resolution displays has greatly increased. These TFT-LCDs inevitably require smaller pixels and narrower spaces between a pixel electrode and neighbouring bus lines, thereby leading to complicated lateral fields near the edge of the pixel [1, 2]. Therefore, in practical cases, one-dimensional modelling, in which uniform electric fields within the pixel region are assumed, is not sufficient and more sophisticated simulation is required to perform optical design for the material parameters and device structures of TFT-LCDs. In recent years, two-dimensional or three-dimensional analyses on lateral fields and director distribution profiles have been extensively performed; consequently generation, movement, and disappearance of the disclination lines caused by lateral fields have been clearly explained [3–8]. However, most reports are concerned with the optical problems of light leakage due to disclination lines, and reports related to the electrical phenomena due to lateral fields are very few.

In this paper, we present a novel method to calculate pixel and inter-electrode capacitances of TFT-LCDs affected by lateral fields, using three-dimensional director and potential profiles. The capacitances are very important parameters for the optimal design of TFT structures and driving waveforms, since the pixel capacitance significantly affects the charging characteristics of the TFTs, and the inter-electrode capacitances seriously distort the voltage waveforms applied to the gate and data electrodes. For the calculation, we first outline a computer simulation of three-dimensional director and potential distribution profiles, and from them calculate the electrostatic energy stored within the pixel. From the electrostatic energy, we can finally obtain the pixel and inter-electrode capacitances.

*Author for correspondence; e-mail: wspark@inha.ac.kr

2. Basic concept of modelling

For liquid crystals, the mean value of the direction of the molecular long axes can be described, as a function of position, by the director $\mathbf{n}(x, y, z)$ of a unit vector. The theoretical model adopted here, for analysing the dynamic behaviour of the director distribution, is based on the Erickson–Leslie theory neglecting the inertial momentum of the molecules [6]. Applying the Gibbs free energy density f_g to the Erickson–Leslie formulation, we obtain

$$\gamma \frac{\partial}{\partial t} n_i = -[f_g]_{n_i} + \lambda n_i, \quad i = \{x, y, z\} \tag{1}$$

where γ is a rotational viscosity, n_i is the cartesian component of the molecular director $\mathbf{n}(x, y, z)$, λ is a

Liquid Crystals ISSN 0267-8292 print/ISSN 1366-5855 online © 2003 Taylor & Francis Ltd
http://www.tandf.co.uk/journals
DOI: 10.1080/0267829021000018077

Lagrange multiplier introduced to maintain the director as a unit vector $|\mathbf{n}| = 1$, and $[f_g]_{n_i}$ is the Euler–Lagrangian equation defined by

$$[f_g]_{n_i} = \frac{\partial f_g}{\partial n_i} - \frac{d}{dx}\left(\frac{\partial f_g}{\partial n_{i,x}}\right) - \frac{d}{dy}\left(\frac{\partial f_g}{\partial n_{i,y}}\right) - \frac{d}{dz}\left(\frac{\partial f_g}{\partial n_{i,z}}\right). \tag{2}$$

The Gibbs free energy density f_g is given as $f_g = f_s - f_e$, where f_s and f_e stand for a strain energy density and an electric energy density, respectively. Here, the strain energy density is expressed as

$$f_s = \left(-\frac{K_{11}}{12} + \frac{K_{22}}{4} + \frac{K_{33}}{12}\right) G_1^{(2)} + \left(\frac{K_{11} - K_{22}}{2}\right) G_2^{(2)} + \left(\frac{K_{33} - K_{11}}{4}\right) G_6^{(3)} + q_0 K_{22} G_4^{(2)} \tag{3}$$

under the assumption of a negligible surface term [6]. In equation (13), K_{11}, K_{22} and K_{33} represent splay, twist and bend elastic constants of the liquid crystals, respectively; q_0 stands for the chirality of the liquid crystals. The G's are represented as

$$G_1^{(2)} = Q_{ij,k} Q_{ij,k}, \quad G_2^{(2)} = Q_{ij,j} Q_{ik,k}, \quad G_4^{(2)} = e_{ijk} Q_{il} Q_{jl,k}, \quad G_6^{(3)} = Q_{ij} Q_{kl,i} Q_{kl,j} \tag{4}$$

where the convention of summing over repeated indices is used, e_{ijk} is a permutation symbol, and the order tensor Q_{ij}'s are expressed as $Q_{ij} = n_i n_j - \delta_{ij}/3$ for the director $\mathbf{n}$ [9]. The electric energy density f_e is given by [7]

$$f_e = \frac{1}{2} \varepsilon_0 \phi_{,l} \varepsilon_{lm} \phi_{,m} \tag{5}$$

where $\phi(x, y, z)$ is the potential distribution, ε_0 is the permittivity of free space; ε_{lm} is the permittivity tensor of liquid crystals expressed as $\varepsilon_{lm} = \varepsilon_\perp \delta_{lm} + (\varepsilon_\parallel - \varepsilon_\perp) n_l n_m$, where $\varepsilon_\parallel$ and $\varepsilon_\perp$ are the parallel and perpendicular dielectric constants of the liquid crystals, respectively.

By substituting equations (3) and (5) into equation (1), we get the dynamic equation of continuum theory for the director as follows:

$$\gamma \frac{\partial n_i}{\partial t} = \left\{ \frac{1}{3}(-K_{11} + 3K_{22} + K_{33})(n_j Q_{ji,ll}) + (K_{11} - K_{22}) n_j (Q_{il,lj} + Q_{jl,li}) + \left(\frac{K_{33} - K_{11}}{2}\right) \times n_j [(2Q_{lm,m} Q_{ji,l} + 2Q_{lm} Q_{ji,lm} - Q_{lm,i} Q_{lm,j})] + 2q_0 K_{22} n_j (e_{iml} Q_{lj,m} + e_{jml} Q_{li,m}) + \varepsilon_0 (\varepsilon_\parallel - \varepsilon_\perp) n_j \phi_{,j} \phi_{,i} \right\} + \lambda n_i \tag{6}$$

where the electric potential distribution $\phi(x, y, z)$ can be obtained by computing the following Laplace equation derived from the Maxwell's equation:

$$(\varepsilon_{ij} \phi_{,j})_{,i} = 0. \tag{7}$$

Calculating the director and potential distributions from equations (6) and (7) is a highly complicated problem due to the dielectric anisotropy of liquid crystals and the resultant coupling between the director and the electric field.

Now we will describe an effective way to obtain all the capacitances existing within a TFT-LCD pixel, using the director and potential distribution profiles. Assuming that imaginary voltages are applied to all the electrodes within a calculation domain and the director distribution is fixed irrelevantly to the imaginary voltages, the electrostatic energy can be calculated using a temporal potential distribution $\varphi(x, y, z)$ determined by the imaginary voltages and the fixed director distribution:

$$W_E = \frac{1}{2} \varepsilon_0 \int_{Vol} (\varphi_{,l} \varepsilon_{lm} \varphi_{,m}) \, dv - \frac{1}{2} \varepsilon_0 \int_S \varphi (\varepsilon_{lm} \varphi_{,m}) \, ds_l \tag{8}$$

where the volume Vol and surface S are the whole volume of the calculation domain and the entire surface enclosing the volume Vol, respectively. The second term of the right hand side in equation (8) is taken into consideration because the calculation domain is restricted to a finite area, that is, a pixel area. The temporal potential distribution $\varphi(x, y, z)$ is also found from the Laplace equation of equation (7) and given boundary conditions.

An alternative approach for obtaining the electrostatic energy is to use the pixel and inter-electrode capacitances existing within the calculation domain:

$$W_E = \frac{1}{2} \sum_{i=1}^{N} \sum_{j>i}^{N} C_{ij} V_{ij}^2, \tag{9}$$

where N is the number of the electrodes in the calculation domain, and $V_{ij} = V_i - V_j$, V_i and V_j being the imaginary voltages applied to i and j electrodes, respectively. Thus, once the electrostatic energy for the imaginary voltages is calculated from equation (8), all the capacitances in the calculation domain can be readily determined from equation (9).

3. Numerical simulation

To obtain the director distribution profile, we have to simulate equations (6) and (7) coupled each other by the director and potential. As the equations are highly non-linear, we adopt an iterative procedure separated in two steps as illustrated in figure 1. We alternate between the solution for the potential while assuming a given director distribution and the solution for the director when the potential distribution is known, until the

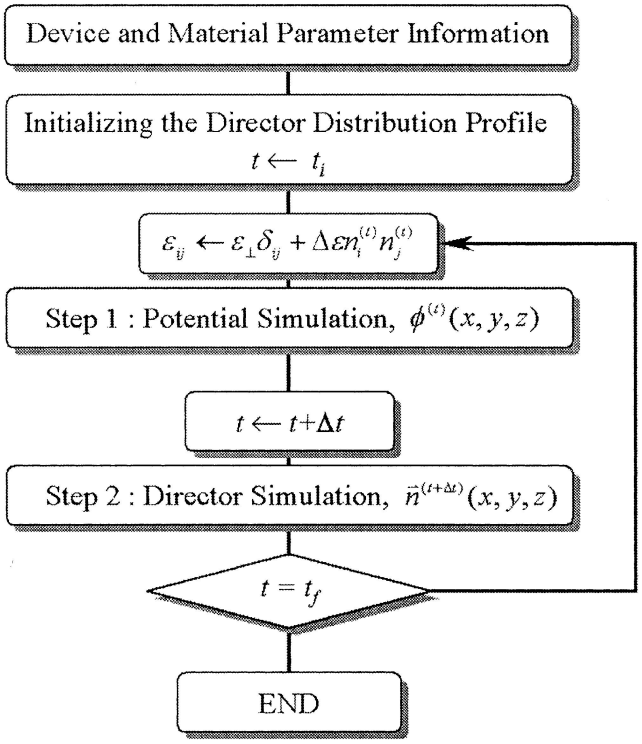

Figure 1. Iterative simulation procedure to obtain the director and potential distribution profiles. Iteration between steps 1 and 2 is performed until a steady state of the director and potential distributions is reached.

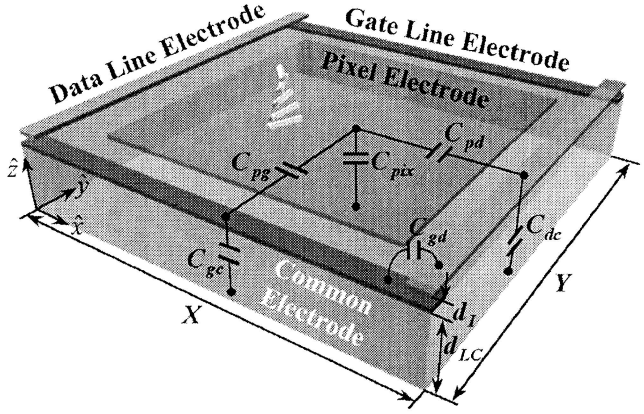

Figure 2. Pixel structure used in the simulation. The pixel area is $60 \times 60\,\mu m^2$. The size of the calculation domain is $80 \times 80\,\mu m^2$ including half of the gate and data bus line width. The spacing between the pixel electrode and the bus lines is 6 μm; the thicknesses of the insulator and the liquid crystal layer, d_I and d_{LC} are 0.2 and 5 μm, respectively. The directors on the top and bottom surfaces are aligned with a pretilt of 2°. The pixel and inter-electrode capacitances are also schematically described.

Table 1. List of the physical parameters for liquid crystal and insulator used in the simulation.

Physical parameter	Value
Liquid crystal	
Perpendicular dielectric constant $\varepsilon_\perp$	3.0
Parallel dielectric constant $\varepsilon_\parallel$	10.0
Rotational viscosity γ	0.12/Pa s
Splay elastic constant K_{11}	10.0×10^{-12}/N
Twist elastic constant K_{22}	7.0×10^{-12}/N
Bend elastic constant K_{33}	13.0×10^{-12}/N
Insulator	
Dielectric constant ε_I	3.0

iterative process reaches a steady state. As a numerical technique, we use a finite difference method (FDM), since the equations are highly non-linear and complicated due to the anisotropy of the elastic constants of liquid crystals. Here we use homogeneous grid spacing for spatial derivatives due to the complexity of a computational geometry and boundary conditions. We also use an explicit method in time domain for numerical calculation, since the non-linearity of the equations of motion for liquid crystals raises troublesome problems when adopting an implicit method. In the case of strong anchoring as assumed here, the directors at boundary surfaces are fixed and specified by rubbing directions and pretilt angles (see figure 2). Neumann boundary conditions are applied to the ends of the z-axis in the calculation domain to reduce computational memories and time, and periodic boundary conditions are employed at the ends of x- and y-axes because of an infinitely repeated pixel structures in the xy-plane [7]. The structure of a pixel is described in figure 2. The material parameters of the insulator and liquid crystal used in the calculation are summarized in table 1.

Figures 3(*a*) and 3(*b*) show the computational results of the three-dimensional director distribution and equipotential contour under an applied voltage of 5 V. It can be seen that an L-shaped disclination line, is formed along the x- and y-axes in the vicinity of the edge of the pixel electrode.

Relating to the capacitances, since the boundary conditions in the xy-plane are repeated periodically, the practical number of electrodes in the calculation domain shrinks to 4, which produces 6 inter-electrode capacitances as schematically shown in figure 2. Therefore, in order to solve for the 6 unknown capacitances, we have to establish six linearly independent equations from the following equation given by equations (8) and (9):

$$\frac{1}{2}\sum_{i=1}^{4}\sum_{j>i}^{4} C_{ij}V_{ij}^2 = \frac{1}{2}\varepsilon_0 \int_{Vol} (\varphi_{,l}\varepsilon_{lm}\varphi_{,m})\,\mathrm{d}v - \frac{1}{2}\varepsilon_0 \int_S \varphi(\varepsilon_{lm}\varphi_{,m})\,\mathrm{d}s_l. \qquad (10)$$

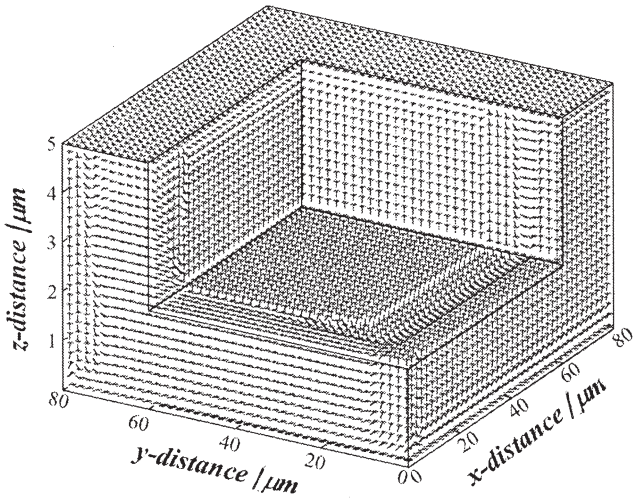

(*a*)

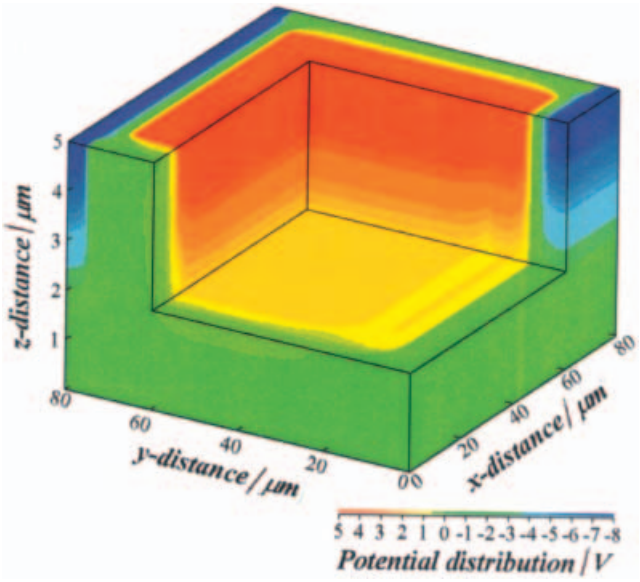

(*b*)

Figure 3. 3-dimensional (a) director distribution and (b) equipotential contour under an applied voltage of 5V. The pixel, gate, data, and common electrodes are biased at 5V, −8V, 0.1V, and 0V, respectively.

The relationship between the numerical notations in equation (10) and the physical parameters in figure 2 for the capacitances is summarized in table 2. To calculate the total electric energy described by the right hand side of equation (10), we first imagine arbitrary voltages to the 4 electrodes, and then compute the potential distribution under this voltage configuration. These voltages constitute the coefficients of the 6 unknown values, C_{ij}'s. By repeating this procedure six times, we can obtain 6×6 coefficient matrix composed of V_{ij}^2's and 6×1 electric energy matrix. The resultant linear system matrix

Table 2. List of capacitance parameters.

Numerical notation	Physical parameter	Corresponding capacitance
C_{12}	C_{pix}	pixel-common capacitance
C_{13}	C_{pg}	pixel-gate capacitance
C_{14}	C_{pd}	pixel-data capacitance
C_{23}	C_{gc}	gate-common capacitance
C_{24}	C_{dc}	data-common capacitance
C_{34}	C_{gd}	gate-data capacitance

is expressed as follows:

$$\frac{1}{2}\begin{bmatrix} {}^{(1)}V_{12}^2 & {}^{(1)}V_{13}^2 & {}^{(1)}V_{14}^2 & {}^{(1)}V_{23}^2 & {}^{(1)}V_{24}^2 & {}^{(1)}V_{34}^2 \\ {}^{(2)}V_{12}^2 & {}^{(2)}V_{13}^2 & {}^{(2)}V_{14}^2 & {}^{(2)}V_{23}^2 & {}^{(2)}V_{24}^2 & {}^{(2)}V_{34}^2 \\ {}^{(3)}V_{12}^2 & {}^{(3)}V_{13}^2 & {}^{(3)}V_{14}^2 & {}^{(3)}V_{23}^2 & {}^{(3)}V_{24}^2 & {}^{(3)}V_{34}^2 \\ {}^{(4)}V_{12}^2 & {}^{(4)}V_{13}^2 & {}^{(4)}V_{14}^2 & {}^{(4)}V_{23}^2 & {}^{(4)}V_{24}^2 & {}^{(4)}V_{34}^2 \\ {}^{(5)}V_{12}^2 & {}^{(5)}V_{13}^2 & {}^{(5)}V_{14}^2 & {}^{(5)}V_{23}^2 & {}^{(5)}V_{24}^2 & {}^{(5)}V_{34}^2 \\ {}^{(6)}V_{12}^2 & {}^{(6)}V_{13}^2 & {}^{(6)}V_{14}^2 & {}^{(6)}V_{23}^2 & {}^{(6)}V_{24}^2 & {}^{(6)}V_{34}^2 \end{bmatrix} \times \begin{bmatrix} C_{12} \\ C_{13} \\ C_{14} \\ C_{23} \\ C_{24} \\ C_{34} \end{bmatrix} = \begin{bmatrix} {}^{(1)}W_{\mathrm{E}} \\ {}^{(2)}W_{\mathrm{E}} \\ {}^{(3)}W_{\mathrm{E}} \\ {}^{(4)}W_{\mathrm{E}} \\ {}^{(5)}W_{\mathrm{E}} \\ {}^{(6)}W_{\mathrm{E}} \end{bmatrix} \tag{11}$$

where the upper script (k) of ${}^{(k)}V_{ij}^2$ means the k'th voltage configuration, and ${}^{(k)}W_{\mathrm{E}}$, the total electric energy for the k'th voltage configuration.

Figure 4 shows the dynamic capacitances as a function of time after a voltage is applied. It is obvious from figure 4 that the pixel capacitance obtained from the three-dimensional method is larger than that from one-dimensional method, and the difference between the two increases markedly with time. This may be explained as follows: in the case of the conventional approach, we cannot predict the director distribution of the liquid crystal outside the pixel electrode, or its dynamic behaviour, due to the lateral fields, and therefore cannot take into consideration quantitatively their effects on the pixel capacitance. Moreover, since the liquid crystal outside the pixel electrode also rises up along the lateral fields formed in the vicinity of the edge of the pixel electrode, the difference between one- and three-dimensional capacitance increases gradually according to the movement of the liquid crystal with time. At a steady state, the pixel capacitance obtained from the three-dimensional approach

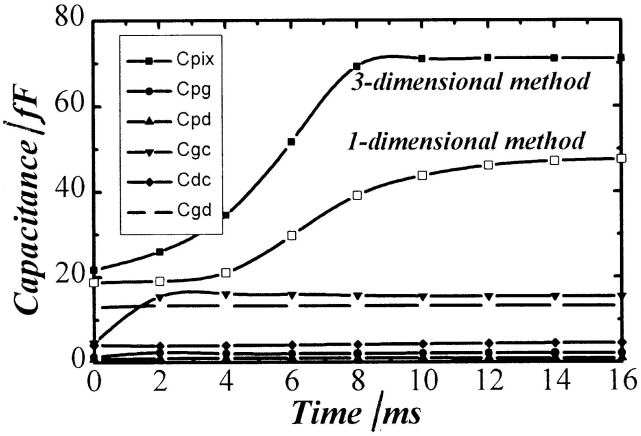

Figure 4. Pixel and inter-electrode capacitances calculated from three-dimensional simulation. For comparison, the pixel capacitance obtained from one-dimensional approach is also plotted.

is shown to be about 40% larger than that from the one-dimensional method. The other inter-electrode capacitances are also depicted in figure 4; in particular, the gate-common and gate-data inter-electrode capacitances have proven to have considerably large values. Therefore, these capacitances must be considered in the optimal design of fine-pitch TFTs and driving waveforms.

4. Conclusions

We have presented a novel method for obtaining pixel and inter-electrode capacitances of TFT-LCDs using three-dimensional director and potential distributions. The model for the Gibbs free energy of a liquid crystal is based on the tensorial form in order to maintain the equivalence of **n** and $-\mathbf{n}$. To describe practical situations, the liquid crystal is treated as having an anisotropic elastic constant. The numerical technique used here is an FDM which is known to be effective for non-linear and complicated problems.

As a result, we have confirmed that the pixel capacitance obtained from the three-dimensional method is about 40% larger than that from the one-dimensional method and a gap between the two values increases markedly with time. In particular among the other inter-electrode capacitances, the gate-common and gate-data inter-electrode capacitances show considerably large values. Therefore, these capacitances must be taken into account in the optimal design of fine-pitch TFTs and driving waveforms.

This work was supported by the IMT2000 program of the Ministry of Science and Technology (MOST) and Ministry of Information and Communication (MIC) of Korea.

References

[1] Kilian, A., and Hess, S., 1989, *Z. Naturforsch*, **44a,** 693.
[2] Onozawa, T., 1990, *Jpn. J. appl. Phys.*, **29,** 1853.
[3] Lien, A., and John, R. A., 1992, *IBM J. Res. Develop.*, **36,** 51.
[4] Pasquale, F. Di, Fernández, F. A., Day, S. E., and Davis, J. B., 1996, *IEEE Trans. Quantum Electron.*, **2,** 128.
[5] Anderson, J. E., Bos, P. J., Cai, C., and Lien, A., 1999, *SID int. Symp. Dig. tech. Pap.*, 628.
[6] Dickmann, S., Escher, J., Cossalter, O., and Mlynski, D. A., 1993, *SID int. Symp. Dig. tech. Pap.*, 638.
[7] Kitamura, M., 1995, *SID int. Symp. Dig. tech. Pap.*, 540.
[8] Kimura, M., Ozawa, T., and Inoue, S., 2000, *IEICE Trans. Electron.*, **E83-C**, 513.
[9] Berreman, D. W., and Meiboom, S., 1984, *Phys. Rev. A.*, **30,** 1955.